S-matrix theory for transmission through billiards in tight-binding approach

2003 J. Phys. A: Math. Gen. 36 11413

(http://iopscience.iop.org/0305-4470/36/45/005)

INSTITUTE OF PHYSICS PUBLISHING JOURNAL OF PHYSICS A: MATHEMATICAL AND GENERAL

J. Phys. A: Math. Gen. **36** (2003) 11413–11433 PII: S0305-4470(03)62707-1

S-matrix theory for transmission through billiards in tight-binding approach

Almas F Sadreev[1,2] **and Ingrid Rotter**[3]

[1] Kirensky Institute of Physics, 660036, Krasnoyarsk, Russia
[2] Department of Physics and Measurement Technology, Linköping University, S-581 83 Linköping, Sweden
[3] Max-Planck-Institut für Physik Komplexer Systeme, D-01187 Dresden, Germany

E-mail: almsa@ifm.liu.se, almas@tnp.krasn.ru and rotter@mpipks-dresden.mpg.de

Received 24 April 2003
Published 29 October 2003
Online at stacks.iop.org/JPhysA/36/11413

Abstract

In the tight-binding approximation we consider multi-channel transmission through a billiard coupled to leads. Following Dittes we derive the coupling matrix, the scattering matrix and the effective Hamiltonian, but take into account the energy restriction of the conductance band. The complex eigenvalues of the effective Hamiltonian define the poles of the scattering matrix. For some simple cases, we present exact values for the poles. We derive also the condition for the appearance of double poles.

PACS number: 03.65.Nk

1. Introduction

In recent years, ballistic transport through quantum systems has been studied as a scattering problem on billiards (microwave cavities) with infinitely high potential walls (hard wall approximation). The scattering properties of such billiards are closely related to the spectral properties of the corresponding closed billiards [1, 2]. The opening of the billiards is realized by attaching at least one lead to them. However, for the study of the transmission through the billiard two leads are necessary. The fundamental object that characterizes the process of quantum scattering is the unitary S-matrix relating the amplitudes of incoming waves to the amplitudes of outgoing waves. Provided that the properties of the Hamiltonian H_B for the closed billiard are known, one can consider its open counterpart and work out the S-matrix formalism by standard methods of the theory of quantum scattering [3–9]. As a result, the S-matrix is expressed in terms of both the Hamiltonian H_B and the matrix elements describing the coupling of the billiard states to the lead states. The explicit expressions for the coupling matrix elements were first formulated in 1996 by Šeba *et al* [10, 11] for the case of point contacts of the leads with the billiard. Later, Fyodorov and Sommers [7] developed their theory for the

connection of the billiard with one lead of finite width by using Neumann boundary conditions (see also [2]). Recently, Dittes [8] considered the same type of open system and derived the expressions for the coupling matrix with Neumann or Dirichlet boundary conditions both by using the Green function technique.

In the present paper, we consider a d-dimensional billiard connected to leads by using another approach that is based on the tight-binding model. The motivation for this consideration is the following. First of all, the increasing development of fabrication techniques requires the possibility to perform reliable numerous experiments on ballistic transport through devices of atomic size [12, 13] and through molecular devices consisting of very few atoms. Secondly, Pichugin *et al* [14] who applied the formula for the coupling matrix derived by Dittes [8], found that their results do not coincide with those of a direct numerical computation of the S-matrix poles, above all for the Dirichlet boundary conditions. As we will show in the present paper, one of the reasons for this disagreement is that the formal continuous approach used by Dittes [8] is unbounded in energy and gives zero radiation shift. In electron transmission through electron wires, however, the energy of the electrons is bounded in energy, at least from below. This fact gives rise to radiation shifts of poles of the S-matrix which cannot be neglected in calculations for concrete systems. Thirdly, it is desirable to receive numerical results from an S-matrix computation within the tight-binding model in order to compare them with the results of numerical computation of the transmission through billiards. With this aim we derive, in the present paper, the coupling matrix, the effective Hamiltonian and the poles of the S-matrix within the tight-binding model and present some typical numerical results.

Here, the following remark should be added. The computer simulations solve the Schrödinger equation using finite-difference Hamiltonians, i.e. the tight-binding approximation. After matching the incoming and outgoing waves with the solutions of the Schrödinger equation by applying the boundary conditions at the transverse sections of the leads, the conductance of the billiard as well as the scattering wavefunction can be computed. Today, the calculations can be performed with a very high accuracy by using large grids and the technique of sparse matrices. The current S-matrix theory is adequate to these computer simulations. It is, however, numerically more time consuming because the effective Hamiltonian is not a sparse matrix. Nonetheless, calculations with the effective Hamiltonian are useful since they provide another view of the results. In this formalism, the resonant peaks of the conductance are related to the poles of the S-matrix that correspond to the eigenvalues of the effective Hamiltonian. It is possible therefore to draw some conclusions on the origin of the resonant peaks and on their possible control by means of external parameters.

In the present paper we will follow, as closely as possible, the Dittes review [8], even in the notation. In the case of microwave or quantum semiconductor billiards, the waves are incident to the billiard through (infinitely) long, straight waveguides (leads) of a certain width. The different channels correspond therefore to different transverse modes of the wave propagation within the leads [2]. At a given frequency E (the Fermi energy), we enumerate the propagating modes by $p = 1, \ldots, M$. Thereby, we associate with the lead region a continuous set of states $|C, p, E\rangle$ where C specifies the lead number (terminal). In the present paper, we consider mostly two leads, the right lead with incident and reflected waves and the left lead with outgoing waves as shown in figure 1. Our approach can, however, be easily generalized to a larger number of leads as done in sections 4 and 5.

2. One-dimensional tight-binding model of resonant tunnelling

A numerical scheme for the computation of quantum transport through billiards with attached leads is mainly based on the finite-difference Schrödinger equation. Applying the Ando

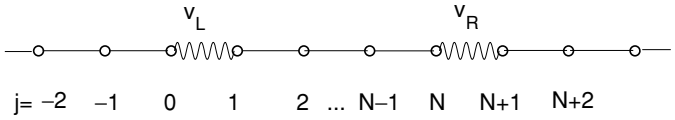

Figure 1. The one-dimensional tight-binding model. The wave lines couple the left and right leads with the box containing N points and, correspondingly, N resonant states.

procedure [15] for the boundary conditions has enabled us to find the transmission properties of the billiards from the scattering wavefunction for any geometry of billiards and straight leads. In order to compare the results from such a computation with the S-matrix theory, we consider systems projected on a lattice with finite grid.

As a first example, we consider a simple one-dimensional model for quantum scattering and transport. This model is formulated as the tight-binding model (the Anderson model)

$$H = -\sum t_j |j\rangle\langle j+1| + \text{c.c.} \tag{1}$$

Here j runs over all sites of the system including left and right leads and the one-dimensional box consisting of N sites as shown in figure 1. The couplings between the box and leads can be governed by adding into (1) the barrier potential $w_L[\delta(j)+\delta(j-1)]+w_R[\delta(j-N)+\delta(j-N-1)]$ which defines the double barrier structure provided that all hopping matrix elements $t_j = 1$. For the limit $w_L, w_R \to \infty$ the box is closed, while for the limit $w_L, w_R \to 1$ the box is completely open. However, it is easier to realize the openness of the box by varying the hopping matrix elements between the leads and the box as follows. We define $t_j = v_L$, if $j = 1$ and $t_j = v_R$, if $j = N$, and $t_j = 1$ otherwise. Then the tight-binding model (1) presents the simplest case of a one-dimensional box with N sites coupled with left and right semi-infinite leads via the corresponding coupling constants v_L, v_R as shown in figure 1. For the limit $v_L, v_R \to 0$ the box is closed, while for the limit $v_L, v_R \to 1$ it is completely open.

The hopping matrix elements t_j in the Hamiltonian (1) are proportional to overlapping integrals of electron wavefunctions of adjacent atoms. The model being similar to the one-dimensional model with a double barrier structure [16, 17], describes resonant tunnelling. In this case the variables $1/v_L, 1/v_R$ play the role of the heights of the double barrier structure provided that $v_L < 1, v_R < 1$. The present model, however, also gives the possibility of considering the case of strong coupling, $v_L > 1, v_R > 1$.

At the left of the box we present the solution of the Schrödinger equation

$$H|\psi\rangle = E|\psi\rangle \tag{2}$$

as

$$\psi_j = \mathrm{e}^{\mathrm{i}kj} + r\mathrm{e}^{-\mathrm{i}kj} \qquad j < 1 \tag{3}$$

where r is the reflection coefficient with energy

$$E(k) = -2\cos k \qquad -\pi \leqslant k \leqslant \pi. \tag{4}$$

As will be seen later, the energy $E(k)$ forms the conduction band $-2 \leqslant E \leqslant 2$ with finite width. At the right of the box we write

$$\psi_j = t\,\mathrm{e}^{\mathrm{i}kj} \qquad j > N. \tag{5}$$

At last, the solution of (2) inside the box is

$$\psi_j = a\,\mathrm{e}^{\mathrm{i}kj} + b\,\mathrm{e}^{-\mathrm{i}kj} \qquad j = 1, 2, \ldots, N. \tag{6}$$

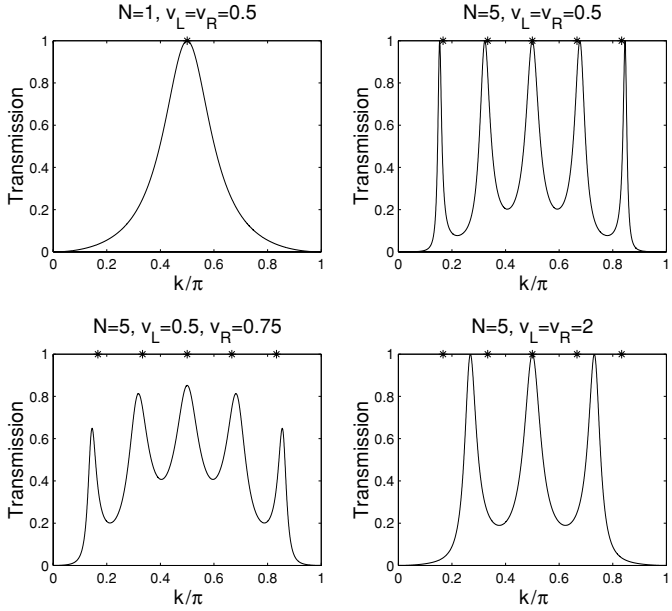

Figure 2. The transmission probability versus the wave number of the incident quantum particle. The positions of the eigenvalues of the closed billiard ($v_L = v_R = 0$) are shown by stars. One can see the radiation shifts caused by the coupling of the 1D box with the leads.

Substituting these functions into (2) we obtain the following linear equations

$$\begin{aligned} &r(\mathrm{e}^{\mathrm{i}k} - E) + v_L\,\mathrm{e}^{\mathrm{i}k}a + v_L b\,\mathrm{e}^{-\mathrm{i}k} = \mathrm{e}^{\mathrm{i}k} \\ &v_L r + \mathrm{e}^{\mathrm{i}k}(\mathrm{e}^{\mathrm{i}k} - E)a + \mathrm{e}^{-\mathrm{i}k}(\mathrm{e}^{-\mathrm{i}k} - E)b = -v_L \\ &\mathrm{e}^{\mathrm{i}kN}(\mathrm{e}^{-\mathrm{i}k} - E)a + \mathrm{e}^{-\mathrm{i}kN}(\mathrm{e}^{\mathrm{i}k} - E)b + v_R\,\mathrm{e}^{\mathrm{i}k(N+1)}t = 0 \\ &v_R\,\mathrm{e}^{\mathrm{i}kN}a + v_R\,\mathrm{e}^{-\mathrm{i}kN}b + \mathrm{e}^{\mathrm{i}k(N+1)}(\mathrm{e}^{\mathrm{i}k} - E)t = 0. \end{aligned} \tag{7}$$

The coefficients a and b can be expressed via the transmission coefficient t as follows

$$a = t\frac{v_R - \frac{1}{v_R}\,\mathrm{e}^{-2\mathrm{i}k}}{1 - \mathrm{e}^{-2\mathrm{i}k}} \qquad b = t\frac{\left(v_R - \frac{1}{v_R}\right)\mathrm{e}^{2\mathrm{i}kN}}{1 - \mathrm{e}^{-2\mathrm{i}k}}. \tag{8}$$

Finally, one obtains

$$\begin{aligned} &t = 4\sin^2 k/A \\ &r = \frac{t}{v_L(1 - \mathrm{e}^{-2\mathrm{i}k})}\left[v_R - \frac{1}{v_R}\,\mathrm{e}^{-2\mathrm{i}k} + \left(\frac{1}{v_R} - v_R\right)\mathrm{e}^{2\mathrm{i}kN}\right] - 1 \end{aligned} \tag{9}$$

for the solution of the system of equations (7) where

$$A = \left(v_L - \frac{1}{v_L}\right)\left(v_R - \frac{1}{v_R}\right)\mathrm{e}^{2\mathrm{i}kN} - \mathrm{e}^{-2\mathrm{i}k}\left(v_L\,\mathrm{e}^{2\mathrm{i}k} - \frac{1}{v_L}\right)\left(v_R\,\mathrm{e}^{2\mathrm{i}k} - \frac{1}{v_R}\right).$$

For the particular case $v_L = v_R = 1$, we obtain from (9) that $t = 1$ and $r = 0$. A typical resonant transmission through a one-dimensional box is shown in figure 2.

The tight-binding model (1) demonstrates a few remarkable features. The first one is the symmetry of the resonant transmission relative to $v_{L,R} \to 1/v_{L,R}$. This symmetry means the following: for small as well as for large coupling coefficients, the effective coupling of the box

to the leads is small. Such a feature was first observed in reactions on atomic nuclei, see the review [6], and analytically derived by Dittes *et al* for an N-level system coupled to one open channel [18]. With increasing coupling strength, the widths of $N-1$ resonance states decrease as $1/v$ in the single-channel case while only one resonance state accumulates almost the total sum of the widths. In our case, the N-level system is coupled to two open channels. Correspondingly, with increasing coupling coefficients v_L, v_R the widths of $N-2$ resonance states decrease while the widths of two resonance states increase. We will return to this feature below when the poles of the scattering matrix will be considered. The second feature is that the heights of the resonant peaks are equal to one only when $v_L = v_R$, similar to the double barrier resonant structure. This fact was firstly established by Ricco and Azbel [17]. The radiation shifts of the positions of the resonant peaks relative to the eigenvalues of the box

$$E_n = -2\cos k_n \qquad k_n = \pi n/(N+1) \qquad n = 1, 2, \ldots, N \tag{10}$$

are the third peculiarity of the tight-binding model. The positions of the eigenvalues (10) are shown in figure 2 by stars. The shifts and widths of the resonant peaks are symmetrical, relative to $k \to -k$, and $E \to -E$. The last symmetry follows from the invariance of the solution of the tight-binding model relative to $t_j \to -t_j$.

3. The S-matrix for the 1D tight-binding model

The simplicity of the model (1) allows us to establish the explicit correspondence between the analytical results for the transmission amplitudes (9) and the S-matrix approach [3–6, 8]. This 1D model was also used in [19] to investigate the width distribution. In this approach the scattering system is decomposed into a closed subsystem described by the internal Hamiltonian H_B with discrete bound states $|\psi_n\rangle$, $n = 1, 2, \ldots, N$ and the continuum of external scattering states $|E, L\rangle$ and $|E, R\rangle$ corresponding to the semi-infinite left and right leads. The Hamiltonian of the two uncoupled subsystems is

$$\begin{aligned} H_0 &= H_B + H_L + H_R & H_B &= \textstyle\sum_n E_n|n\rangle\langle n| \\ H_L &= \int_{-2}^{2} \mathrm{d}E\, E|E, L\rangle\langle E, L| & H_R &= \int_{-2}^{2} \mathrm{d}E\, E|E, R\rangle\langle E, R| \end{aligned} \tag{11}$$

where E_n are the energies of the bound states of the 1D closed billiard, and E denotes the energy of the leads. We use the following normalization conditions

$$\langle n|m\rangle = \delta_{nm} \qquad \langle E, L|E', L\rangle = \langle E, R|E', R\rangle = \delta(E - E'). \tag{12}$$

The couplings between the internal and external subsystems can be incorporated by the coupling operator

$$V = \sum_n \sum_{C=L,R} \int_{-2}^{2} \mathrm{d}E\, V_n(E, C)|E, C\rangle\langle n| + \text{h.c.} \tag{13}$$

As shown in figure 1 the closed 1D billiard consists of N sites with energies given by equation (10) and the corresponding eigenfunctions

$$\psi_n(j) = \sqrt{\frac{2}{N+1}} \sin\left(\frac{\pi n j}{N+1}\right) \qquad j = 1, 2, \ldots, N. \tag{14}$$

These eigenfunctions satisfy the Dirichlet boundary conditions $\psi_n(0) = \psi_n(N+1) = 0$. Since the leads are semi-infinite wires the wavefunctions of the left and right leads are, respectively

$$\psi_{E,L}(j) = \sqrt{\frac{1}{2\pi|\sin k|}} \sin k(1-j) \qquad \psi_{E,R}(j) = \sqrt{\frac{1}{2\pi|\sin k|}} \sin k(j-N). \tag{15}$$

The energy in the leads corresponding to a single conductance energy band, is defined by $E(k) = -2\cos k$, $-\pi \leqslant k \leqslant \pi$. It is easy to see that in the continuous limit $k \to 0$ the functions (15) take the form

$$\psi_{E,L}(x) = \sqrt{\frac{1}{2\pi|k|}}\sin kx \tag{16}$$

given in [7]. From (13) we have

$$V_n(E, C) = \langle E, C|V|n\rangle = \langle E, C|\sum_j |j\rangle\langle j|V|\sum_{j'}|j'\rangle\langle j'|n\rangle \qquad C = L, R.$$

Since as shown in figure 1 the coupling matrix elements $\langle j|V|j'\rangle$ are not equal to zero if only $j = 0, 1$, $j' = 1, 0$ or $j = N, N+1$, $j' = N+1, N$, we obtain finally, using (14) and (15), the coupling coefficients as

$$\begin{aligned} V_n(E, L) &= v_L\psi_{E,L}(0)\psi_n(1) = v_L\sqrt{\frac{\sin k}{\pi(N+1)}}\sin\frac{\pi n}{N+1} \\ V_n(E, R) &= v_R\psi_n(N)\psi_{E,R}(N+1) = v_R\sqrt{\frac{\sin k}{\pi(N+1)}}\sin\frac{\pi nN}{N+1}. \end{aligned} \tag{17}$$

For the total Hamiltonian

$$H = H_0 + V \tag{18}$$

the stationary Schrödinger equation reads

$$H|\psi(E)\rangle = E(k)|\psi(E)\rangle. \tag{19}$$

For $E(k)$ different from the eigenvalues E_n of the box, the operator $(E + \mathrm{i}0 - H_0)V$ is well defined and equation (19) is equivalent to the Lippmann–Schwinger equation

$$|\psi\rangle = |\psi_0\rangle + (E + \mathrm{i}0 - H_0)^{-1}V|\psi\rangle \tag{20}$$

if the boundary condition of outgoing waves is adopted and

$$(E - H_0)|\psi_0\rangle = 0. \tag{21}$$

The Lippmann–Schwinger equation (20) also reads

$$|\psi\rangle = [F(E + \mathrm{i}0)]^{-1}|\psi_0\rangle \tag{22}$$

where

$$F(E + \mathrm{i}0) = 1 - (E + \mathrm{i}0 - H_0)^{-1}V \tag{23}$$

and

$$|\psi_0\rangle = \begin{pmatrix} |E, L\rangle \\ 0 \\ |E, R\rangle \end{pmatrix}. \tag{24}$$

Following [5, 8] we introduce three projection operators: for the left and right leads

$$P_C = \int \mathrm{d}E|E, C\rangle\langle E, C| \tag{25}$$

and for the billiard

$$P_B = \sum_n |n\rangle\langle n| \tag{26}$$

with the help of which we can write the scattering wavefunction (22) as

$$|\psi\rangle = \begin{pmatrix} P_L|\psi\rangle \\ P_B|\psi\rangle \\ P_R|\psi\rangle \end{pmatrix} = \begin{pmatrix} |\psi_L\rangle \\ |\psi_B\rangle \\ |\psi_R\rangle \end{pmatrix}. \tag{27}$$

Then the coupling operator (13) reads

$$V = \begin{pmatrix} P_L V P_L & P_L V P_B & P_L V P_R \\ P_B V P_L & P_B V P_B & P_B V P_R \\ P_R V P_L & P_R V P_B & P_R V P_R \end{pmatrix} = \begin{pmatrix} 0 & V_{LB} & 0 \\ V_{BL} & 0 & V_{BR} \\ 0 & V_{RB} & 0 \end{pmatrix} \tag{28}$$

where by using (17) we obtain

$$\begin{aligned} V_{BL} &= v_L \sum_n \psi_n(1) \sqrt{\frac{1}{2\pi}} \int \mathrm{d}E [1 - (E/2)^2]^{1/4} |n\rangle\langle E, L| \\ V_{BR} &= v_R \sum_n \psi_n(N) \sqrt{\frac{1}{2\pi}} \int \mathrm{d}E [1 - (E/2)^2]^{1/4} |n\rangle\langle E, R| \end{aligned} \tag{29}$$

and $V_{BC} = V_{CB}^+$. Substituting (28) into (23) we have

$$F = \begin{pmatrix} 1 & -\frac{1}{E-H_L} V_{LB} & 0 \\ -\frac{1}{E-H_B} V_{BL} & 1 & -\frac{1}{E-H_B} V_{BR} \\ 0 & -\frac{1}{E-H_R} V_{RB} & 1 \end{pmatrix}. \tag{30}$$

Using the identity

$$\begin{pmatrix} 1 & -A & 0 \\ -B & 1 & -C \\ 0 & -D & 1 \end{pmatrix}^{-1} = \begin{pmatrix} 1 + ATB & AT & ATC \\ TB & T & TC \\ DTB & DT & 1 + DTC \end{pmatrix} \tag{31}$$

one obtains for the inverse matrix F

$$F^{-1} = \begin{pmatrix} 1 + \frac{1}{E-H_L} V_{LB} \frac{1}{D} \frac{1}{E-H_B} V_{BL} & \frac{1}{E-H_L} V_{LB} \frac{1}{D} & \frac{1}{E-H_L} V_{LB} \frac{1}{D} \frac{1}{E-H_B} V_{BR} \\ \frac{1}{D} \frac{1}{E-H_B} V_{BL} & \frac{1}{D} & \frac{1}{D} \frac{1}{E-H_B} V_{BR} \\ \frac{1}{E-H_R} V_{RB} \frac{1}{D} \frac{1}{E-H_B} V_{BL} & \frac{1}{E-H_R} V_{RB} \frac{1}{D} & 1 + \frac{1}{E-H_R} V_{RB} \frac{1}{D} \frac{1}{E-H_B} V_{BR} \end{pmatrix}. \tag{32}$$

where

$$T = \frac{1}{1 - BA - CD}$$

and

$$D = 1 - \frac{1}{E - H_B} \sum_{C=L,R} V_{BC} \frac{1}{E - H_C} V_{CB}. \tag{33}$$

From equations (22) and (27) it follows that the wavefunction in the interior of the billiard is

$$|\psi_B\rangle = Q^{-1} \sum_{C=L,R} V_{BC} |E, C\rangle \tag{34}$$

where

$$Q = E^+ - H_B - \sum_{C=L,R} V_{BC} \frac{1}{E^+ - H_C} V_{CB}. \tag{35}$$

Here we used the identity [8]

$$\frac{1}{1 - AB} A = A \frac{1}{1 - BA}.$$

If we substitute the coupling constants (17) into formula (35), it follows that the matrix elements of the operator (35) can be presented as matrix elements of the effective Hamiltonian [4, 8]

$$\langle m|Q|n\rangle = E^{+}\delta_{mn} - \langle m|H_{\rm eff}|n\rangle \tag{36}$$

where

$$\langle m|H_{\rm eff}|n\rangle = E_m\delta_{mn} + \frac{1}{2\pi}V_{mn}\int_{-2}^{2} {\rm d}E_1 \frac{\sqrt{1-(E_1/2)^2}}{E+{\rm i}0-E_1} = E_m\delta_{mn} - V_{mn}\,{\rm e}^{{\rm i}k}. \tag{37}$$

The last expression was obtained by using the formula

$$\frac{1}{x+{\rm i}0} = {\rm i}\pi\delta(x) + P\frac{1}{x}$$

where P denotes the principal value integral and

$$V_{mn} = v_L^2\psi_m(1)\psi_n(1) + v_R^2\psi_m(N)\psi_n(N). \tag{38}$$

As can be seen from (37), the lattice approach gives rise to a finite shift of the resonant energies

$$F_{mn}(E) = \frac{1}{2N}V_{mn}E \tag{39}$$

which is of the same order of magnitude as the width of the resonant peak of the transmission

$$\gamma_{mn}(E) = \frac{1}{N}V_{mn}\sqrt{1-(E/2)^2}. \tag{40}$$

This energy shift is the main difference between the present tight-binding (lattice) approach and the continuous approach by Dittes [8] where the shifts are equal to zero. The reason for this difference is that the energy is restricted to the conductance band $E = -2\cos k$.

The S-matrix is [5, 8]

$$S_{CC'} = \delta_{CC'} - 2\pi{\rm i}\langle E, C|V_{CB}Q^{-1}V_{BC'}|E, C'\rangle = \begin{pmatrix} r & t' \\ t & r' \end{pmatrix} \tag{41}$$

where r and r' are the reflection coefficients from left to left and from right to right, respectively, and t and t' are the transmission coefficients from left to right and from right to left. Using the definition of the coupling operator (29) we can write the transmission coefficient of the S-matrix (41) as follows

$$t = -2\pi{\rm i}\sum_{mn} V_m(E, L)\langle m|Q^{-1}|n\rangle V_n^*(E, R). \tag{42}$$

A concrete calculation of the transmission coefficient needs the procedure of inversion of the matrix (36). It is therefore more convenient to use a representation by means of the set of eigenstates of the effective Hamiltonian (37) [6, 9]. Using the biorthogonal basis of the effective Hamiltonian

$$H_{\rm eff}|\lambda) = z_\lambda|\lambda) \qquad (\lambda|\lambda') = \delta_{\lambda,\lambda'} \qquad |\lambda) = |\lambda\rangle \qquad (\lambda| = \langle\lambda|^* \tag{43}$$

and the projection operator

$$P_{\rm eff} = \sum_{\lambda} |\lambda)(\lambda| \tag{44}$$

we obtain

$$t = -2\pi{\rm i}\sum_{\lambda} \frac{\langle E, L|V|\lambda)(\lambda|V|E, R\rangle}{E - z_\lambda}. \tag{45}$$

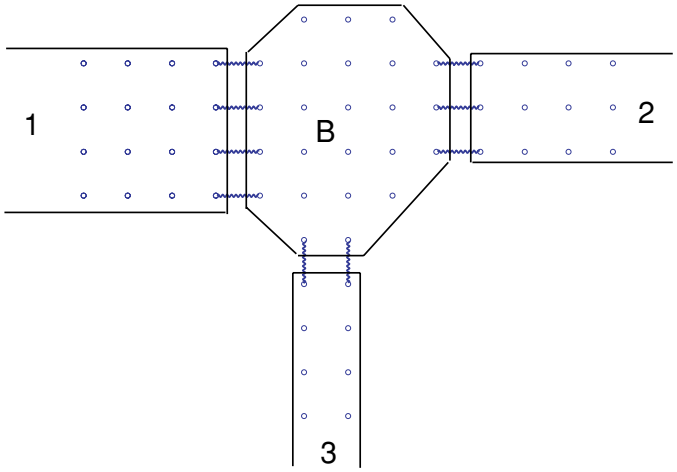

Figure 3. The two-dimensional billiard B attached to three different leads $C = 1, 2, 3$. The coupling coefficients v_C between the leads and the billiard are shown by wave lines.

Equation (45) shows immediately that the eigenvalues z_λ of the effective Hamiltonian define the poles of the scattering matrix. We underline that the coupling coefficients in the pole representation (45) have to be calculated by means of the eigenstates $|\lambda)$ of the effective Hamiltonian but not with the eigenstates $|b\rangle$ of the closed billiard. The importance of this difference is presented in [20].

Let us consider for illustration the limiting case $N = 1$, the one-site Anderson model [19], which corresponds to the 1D box with a single eigenstate. For simplicity we take $v_L = v_R = v$. Then the formula for the transmission coefficient (9) reduces to

$$t = -\frac{\mathrm{i}v^2 \sin k}{\cos k - v^2 \,\mathrm{e}^{\mathrm{i}k}}. \tag{46}$$

On the other hand, from (37) and (38) we have the effective Hamiltonian as the c-number $H_{\mathrm{eff}} = z_1 = E_1 - 2v^2 \,\mathrm{e}^{\mathrm{i}k}$ where for the one-site dot $E_1 = 0$. Moreover, $V_1(E, L) = \tilde{V}_1(E, R) = v\sqrt{\frac{\sin k}{2\pi}}$. Substituting these formulae into (45) we obtain the same formula as (46) with $E = -2\cos k$. An analysis of the S-matrix for the transmission through the N-site 1D box is given in section 5.

4. S-matrix theory for transmission through billiards

Let us consider a d-dimensional billiard specified by the internal eigenstates $|b\rangle$ and eigenvalues E_b,

$$H_B|b\rangle = E_b|b\rangle. \tag{47}$$

Let Ω be the $d-1$ surface of the billiard which encloses the internal region of the billiard B with the points $\mathbf{x} \in B$. The eigenfunctions are $\langle \mathbf{x}|b\rangle = \psi_b(\mathbf{x})$. We assume that M leads are attached to the billiard. Each lead is a tube with arbitrary $d-1$ dimensional cross-section $\omega_C, C = 1, 2, \ldots, M$, and is semi-infinite along the direction $z_C \perp \omega_C$. The geometry of the system is illustrated in figure 3 for the particular two-dimensional case and $M = 3$. We consider that the cross-section of the Cth tube is constant over the z_C-direction. This allows a separation of variables $\mathbf{x}_\perp \in \omega_C$ and z_C.

Assuming that the eigenvalues and eigenfunctions for the transverse section of the Cth lead are known and denoted by $E_{p_C}, \phi_{p_C}(\mathbf{x}_\perp)$, we can write the Schrödinger equation for the leads in the following manner

$$H_C|E, C, p_C\rangle = E|E, C, p_C\rangle. \tag{48}$$

Here

$$E = -2\cos(k_{p_C}) + E_{p_C} \tag{49}$$

$$\psi_{p_C}(\mathbf{x}) = \sqrt{\frac{1}{2\pi|\sin k_{p_C}|}}\sin k_{p_C}(j_z - j_C)\phi_{p_C}(\mathbf{x}_\perp) \tag{50}$$

and j_C is the longitudinal position of the attachment of the Cth lead to the billiard. Then the Hamiltonian of the uncoupled system consisting of the billiard and the M leads is

$$H_0 = \sum_b E_b|b\rangle\langle b| + \sum_{C=1}^{M}\sum_{p_C}\int_{-2+E_{p_C}}^{2+E_{p_C}} \mathrm{d}E\; E|E, C, p_C\rangle\langle E, C, p_C| + \text{h.c.} \tag{51}$$

Similar to (13) let us write the coupling operator as

$$V = \sum_b\sum_C\sum_{p_C}\int_{-2+E_{p_C}}^{2+E_{p_C}} \mathrm{d}E\; V_b(E, C, p_C)|E, C, p_C\rangle\langle b| + \text{h.c.} \tag{52}$$

where

$$V_b(E, C, p_C) = \langle E, C, p_C|V|b\rangle. \tag{53}$$

Let $A_C \subset \Omega$ be the areas at which the leads are attached to the billiard. They terminate the semi-infinite leads at $j_z = j_C$. The shape of A_C is ω_C, the cross-section of the lead. The Cth lead is connected to the billiard through the hopping matrix elements v_C, as shown in figure 3 by wave lines. Substituting (50) into (53), we obtain for the coupling matrix elements

$$V_b(E, C, p_C) = \sum_{\mathbf{x},\mathbf{y}}\psi_{p_C}(\mathbf{x})\langle\mathbf{x}|V|\mathbf{y}\rangle\psi_b(\mathbf{y}) = v_C\sqrt{\frac{|\sin k_{p_C}|}{2\pi}}\sum_{\mathbf{x}_\perp\in A_C}\phi_p(\mathbf{y}_\perp)\psi_b(\mathbf{y}_\perp). \tag{54}$$

It is justified to generalize the one-dimensional case presented in section 2 to the general case with $d > 1$. In the following, we present some formulae that follow in a straightforward manner. Formulae (36) and (37) now read

$$\langle b|Q|b'\rangle = E^+\delta_{bb'} - \langle b|H_{\text{eff}}|b'\rangle \tag{55}$$

where

$$\langle b|H_{\text{eff}}|b'\rangle = E_b\delta_{bb'} - \sum_C\sum_{p_C} W_C(b, p_C)W_C(b', p_C)\,\mathrm{e}^{\mathrm{i}k_{p_C}} \tag{56}$$

and

$$W_C(b, p) = v_C\sum_{\mathbf{x}_\perp\in A_C}\psi_b(\mathbf{x}_\perp)\phi_p(\mathbf{x}_\perp). \tag{57}$$

The number of channels in each lead is defined by the condition $E_{p_C} < E$.

Let us consider the continuous approximation. For simplicity we treat the typical case $d = 2$. Then the leads are stripes as shown in figure 3 with $E_{p_C} = -2\cos(\pi p_C/(N_C + 1)) \approx (\pi p_C/N_C)^2 - 2 = \epsilon_{p_C} - 2$, where N_C is the numerical width of the Cth lead. In the continuous limit $N_C \to \infty$, or $\epsilon_{p_C} \to 0$ for a restricted number of channels. We can write (49) as $E = -2\cos k \approx -2\cos(k_{p_C}) + \epsilon_{p_C} - 2$. In order to present the energy of the incident particle in the usual form $E \approx \epsilon(k) - 2$ with $\epsilon(k) = k^2$ for the continuous case we have to consider

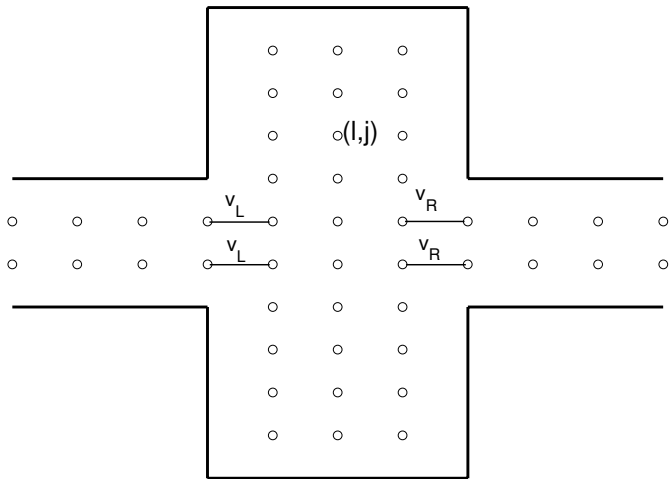

Figure 4. The geometry for the transmission through a rectangular billiard in the tight-binding approach. The couplings v_C between the leads and the billiard are shown by solid lines.

that $k \ll 1$. Substituting these relations into (49) we obtain $\cos(k_{p_C}) \approx (\epsilon_{p_C} - \epsilon(k))/2 \ll 1$. Therefore, we can approximate $e^{ik_{p_C}} \approx (\epsilon_{p_C} - \epsilon(k))/2 + i$. As a result the effective Hamiltonian (56) takes the standard form

$$H_{\text{eff}} \approx \tilde{H}_B - iWW^+ \tag{58}$$

where $\tilde{H}_B$ is the billiard Hamiltonian the eigenenergies of which are corrected by the radiation shifts $(\epsilon_{p_C} - \epsilon(k))WW^+$, and W is the matrix whose elements are given by (57). The dimension of the matrix W is $N \times K$ where N is the number of states in the billiard, and $K = \sum_C \max(p_C)$.

Finally, the S-matrix elements (41) are characterized by the channel numbers and read

$$\langle C, p_C|S|C', p'_{C'}\rangle = \delta_{CC'}\delta_{pp'} - 2\pi i\langle E, C, p_C|V_{CB}Q^{-1}V_{BC'}|E, C', p'_{C'}\rangle. \tag{59}$$

For calculation of the S-matrix we can use the set of the eigenstates ψ_b of the Hamiltonian of the closed billiard, see (42), or the biorthogonal set of eigenstates ψ_λ of the effective Hamiltonian of the open billiard, see (45). In the last case one can see immediately that the poles of the S-matrix correspond to the eigenvalues of the effective Hamiltonian (56).

5. Some applications of the general theory

5.1. Transmission through a 2D rectangular billiard

The typical features of the quantum mechanical transmission through a billiard can be described by means of a two-dimensional billiard with two attached leads of equal widths (figure 4). In the tight-binding formulation $\mathbf{x} = a_0(l, j)$ where a_0 is the lattice unit. The eigenfunctions and eigenvalues of the rectangular billiard are

$$\psi_{m,n}(l, j) = \psi_m(l)\psi_n(j) \tag{60}$$

$$E_{m,n} = E_m + E_n \tag{61}$$

where E_m and ψ_m are defined by equations (10), (14) for the corresponding numerical size of the box N_x, N_y. Further, the wavefunctions (50) of the leads and their energy (49) are

$$\psi_{E,L,p}(l,j) = \sqrt{\frac{1}{2\pi|\sin k_p|}}\sin k_p(1-l)\phi_p(j)$$
$$\psi_{E,R,p}(l,j) = \sqrt{\frac{1}{2\pi|\sin k_p|}}\sin k_p(l-N_x)\phi_p(j) \tag{62}$$

$$E = -2\cos k_p + E_p \qquad E_p = -2\cos\left(\frac{\pi p}{N_L+1}\right) \tag{63}$$

where $p = 1, 2, 3, \ldots$ enumerates the channel number and N_L is the numerical width of the leads. We denote the numerical positions of the lead walls by N_1 and N_2 so that $N_L = N_2 - N_1$. It follows from the geometry of the system that $1 \leqslant N_1 \leqslant N_2 \leqslant N_y$. Therefore, the area of intersection between leads and billiard A_C is a straight line of length N_L. The eigenfunctions in the transverse sections of the leads have the following form

$$\phi_p(j) = \sqrt{\frac{2}{N_L+1}}\sin\left(\frac{\pi p(j-N_1)}{N_L+1}\right). \tag{64}$$

Substituting (60) and (64) into (54) we have for the elements of the coupling matrix

$$V_{m,n}(E,L,p) = v_L\psi_m(1)\sqrt{\frac{|\sin k_p|}{2\pi}}\sum_{j=N_1}^{N_2}\phi_p(j)\psi_n(j)$$
$$V_{m,n}(E,R,p) = v_R\psi_m(N_x)\sqrt{\frac{|\sin k_p|}{2\pi}}\sum_{j=N_1}^{N_2}\phi_p(j)\psi_n(j). \tag{65}$$

Here the Latin indices L, R denote the left and right leads, respectively, as shown in figure 4. The formulae for the effective Hamiltonian (56) with (57) read

$$\langle m,n|H_{\rm eff}|m',n'\rangle = E_{m,n}\delta_{mm'}\delta_{nn'} - v_L^2\psi_m(1)\psi_{m'}(1)\sum_{p}^{\Lambda}W_L(n,p)W_L(n',p)\,{\rm e}^{{\rm i}k_p}$$
$$- v_R^2\psi_m(N_x)\psi_{m'}(N_x)\sum_{p}^{\Lambda}W_R(n,p)W_R(n',p)\,{\rm e}^{{\rm i}k_p} \tag{66}$$

with

$$W_C(n,p) = \sum_{j=N_1}^{N_2}\psi_n(j)\phi_p(j). \tag{67}$$

The number of channels Λ is defined by the condition $\epsilon_p < E$.

Let us now consider the correspondence of the formulae obtained to those received in the continuous approach by Dittes [8]. First it is necessary to choose, in the last case, some characteristic space length. This may be the width of the lead or the size of the billiard. Here we choose, as usual in the literature, the former and denote it by d. In the continuous approach, the eigenfunctions and the eigenvalues of the rectangular billiard (60) take the following form

$$\tilde{\psi}_{m,n}(x,y) = \tilde{\psi}_m(x)\tilde{\psi}_n(y) \qquad \tilde{\psi}_m(x) = \sqrt{\frac{2}{a}}\sin(mx/a) \tag{68}$$

$$\tilde{E}_{m,n} = E_0\pi^2 \left\{ \frac{m^2}{(a/d)^2} + \frac{n^2}{(b/d)^2} \right\} \tag{69}$$

for Dirichlet boundary conditions, where a and b characterize the size of the billiard and $E_0 = \hbar^2/2md^2$. The eigenfunctions and eigenenergies of the leads are

$$\psi_{E,L,p}(x, y) = \sqrt{\frac{1}{\pi d|k|}} \sin(kx) \sin(\pi py/d) \tag{70}$$

$$\tilde{E} = E_0[(\tilde{k}d)^2 + (\pi p)^2]. \tag{71}$$

With $x = a_0 i$, $y = a_0 j$ we find the following relations

$$1 + N_x = a/a_0 \qquad 1 + N_y = b/a_0 \qquad 1 + N_L = d/a_0 \tag{72}$$

from the comparison of (60) and (62) with (68) and (70). In the discrete case $\psi_m(j = 0) = 0$. Therefore, it holds approximately

$$\psi_m(1) = a_0 \frac{\psi_m(1) - \psi_m(0)}{a_0} \approx a_0 \psi'_m(0)$$

for the continuous case, and the coupling matrix elements (53) are

$$V_{m,n}(E, L, p) \approx V_0 \Psi'_{m,n,p}(0) \tag{73}$$

where

$$\Psi_{\alpha,p}(x, y) = \int_{y_1}^{y_2} \mathrm{d}y\, \phi_p(y) \psi_{m,n}(x, y) \qquad V_0 = \sqrt{\frac{1}{2\pi k_p}}$$

and y_1, y_2 are the positions of the lead walls along the y-axis, so that $d = y_2 - y_1$. The same expressions were derived in [8, 10]. In practical numerical computations, these approximations are valid if the half of the wavelength π/k exceeds the numerical lattice unit a_0 by at least a factor 10.

It might seem that, for the continuous limit $a_0 \to 0$, the radiation shifts go to zero and we can use the Weidenmüller–Dittes approach directly. However, as can be seen from (71), the energy is bounded from below. As a consequence, the principal value integral in the matrix elements of the effective Hamiltonian does not vanish. This is different to the assumption in [8] that $\tilde{E}$ has no limits.

5.2. Transmission through a two-site quantum dot

A box consisting of a single atom (site) coupled to a left lead and a right one (L and R continuous) is the simplest case that gives rise to the Breit–Wigner type formula for the transmission amplitude (46) shown in figure 2(*a*). Let us now consider a two-site box that gives rise to a 2×2 effective Hamiltonian. The properties of such Hamiltonians are studied in literature [9] by focusing on double poles of the S-matrix (branch points in the complex energy plane) without relation to a realistic system as well as in relation to laser induced structures in atoms [21]. In our present study, we have the possibility of specifying the effective 2×2 Hamiltonian for another specific system to study its properties and to compare the results with those of the general study.

There are different ways to connect the two cite box with the leads as shown in figure 5. The cases (*a*) and (*b*) are identical, but differ from (*c*).

For the case (*a*) we obtain from (66)

$$H_{\mathrm{eff}} = -\begin{pmatrix} -1 + \lambda & \mu \\ \mu & -1 + \lambda \end{pmatrix} \tag{74}$$

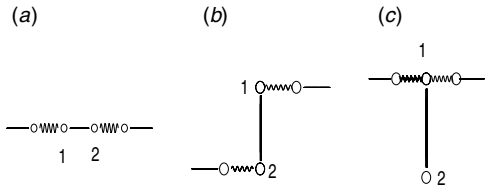

Figure 5. Two-site dot coupled to two leads.

where

$$\lambda = \tfrac{1}{2}\left(v_L^2 + v_R^2\right)\mathrm{e}^{\mathrm{i}k} \qquad \mu = \tfrac{1}{2}\left(v_L^2 - v_R^2\right)\mathrm{e}^{\mathrm{i}k}. \tag{75}$$

The eigenvalues are

$$z_{1,2} = -\lambda \pm \sqrt{1+\mu^2}. \tag{76}$$

They define the poles of the S-matrix as shown in sections 3 and 4. Since the effective Hamiltonian is symmetric but not Hermitian we use the biorthogonal basis [22, 6] normalized by the condition $(m|n) = \delta_{mn}, m = 1, 2, n = 1, 2$ where $(m| \equiv \langle m|^*$. The right eigenstates of (74) are

$$|1\rangle = \begin{pmatrix} a_1 \\ a_2 \end{pmatrix} = \frac{1}{\sqrt{2\eta(\eta+1)}}\begin{pmatrix} -\mu \\ 1+\eta \end{pmatrix} \qquad |2\rangle = \begin{pmatrix} a_2 \\ -a_1 \end{pmatrix}. \tag{77}$$

With the formulae (56), (57) the transmission amplitude takes the form

$$t = \frac{2\mathrm{i}v_L v_R\sqrt{1-(E/2)^2}}{(E-z_1)(E-z_2)}. \tag{78}$$

The S-matrix has a double pole when two of the eigenvalues (76) coincide, i.e. when

$$E = 0 \qquad |\mu| = 1. \tag{79}$$

The energy dependence of the poles (76) is shown in figure 6. Such pole behaviour was shown in many works based on the general presentation of the effective Hamiltonian as a 2×2 matrix (see, for example, review [9]). The cases (*a*) and (*b*) in figure 6 ($|\mu| > 1$) correspond to a free crossing of energy levels in the complex plane, while the cases (*c*) and (*d*) (dashed curves) correspond to the self-avoided crossing.

The case (*c*) in figure 5 gives

$$H_{\mathrm{eff}} = \begin{pmatrix} -1+\lambda & \lambda \\ \lambda & 1+\lambda \end{pmatrix} \tag{80}$$

where λ is given by (75). The poles of the scattering matrix are

$$z_{1,2} = \lambda \pm \sqrt{1+\lambda^2} \tag{81}$$

and the transmission amplitude is given by

$$t = -\frac{2\mathrm{i}v_L v_R E\sqrt{1-(E/2)^2}}{(E-z_1)(E-z_2)}. \tag{82}$$

A double pole of the S-matrix can be found at

$$E = 0 \qquad |\lambda| = 1. \tag{83}$$

The comparison of (82) with (78) shows that the way the leads are connected with the box plays an important role for the conductance. In particular, the connection (*a*) gives rise

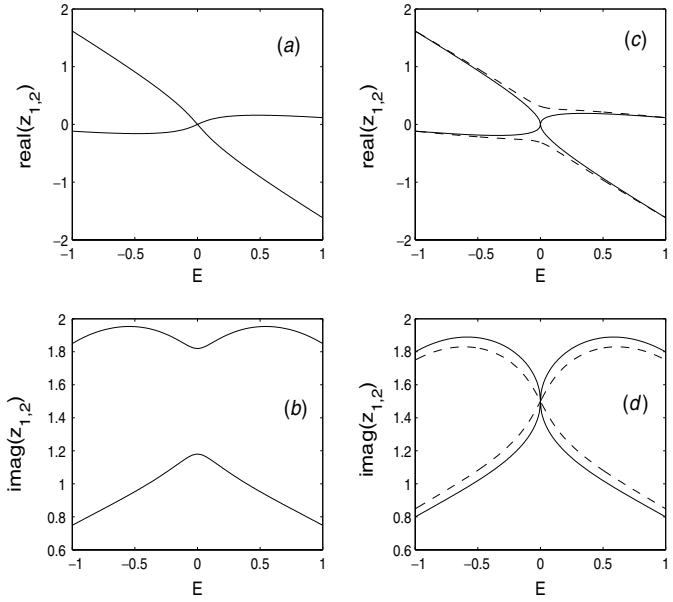

Figure 6. The energy behaviour of the poles for the transmission through the two-site dot shown in figure 5(*a*). (*a*) and (*b*): $|\mu| = 1 + 0.03$. (*c*) and (*d*): $|\mu| = 1 - 0.03$ (dashed curves). The solid curves in (*c*) and (*d*) show the case of a double pole, $|\mu| = 1$.

to a transmission zero only at the edges of the energy band $E = \pm 2$ while the connection (*c*) leads to $t = 0$ at $E = 0$. The energy behaviour of the poles (81) is, however, similar to that of the poles (76) and a double pole of the S-matrix appears at $E = 0$ in both cases. Therefore, the transmission is equal to zero in case (*c*) at the energy where the S-matrix has a double pole while this is not so in the cases (*a*) and (*b*). This shows clearly that the transmission zero for the case (*c*) is an interference effect.

5.3. Transmission through the N-site 1D box

As a next application, we consider the 1D model with N sites presented in figure 1 in order to understand the reduction of the number of transmission peaks by enlarging the coupling coefficients. In figure 2, the resonant transmission has $N = 5$ peaks at small coupling coefficients v_L, v_R but $N - 2$ peaks for large coupling coefficients.

Using formulae (37) and (38), the eigenvalues $z_k, k = 1, 2, \ldots, N$ of the effective Hamiltonian can be found numerically. In figure 7, the real and imaginary parts of the five eigenvalues of the effective Hamiltonian (poles of the S-matrix) are shown versus the coupling constants v_L, v_R for $N = 5$ and $E = 1$. In figures 7(*a*) and (*b*), the right coupling coefficient v_R is chosen to be small. In this case, one of the resonance states is broadened with increasing v_L and becomes shifted beyond the energy band. The incident energy E is tuned to the second energy level $E_2 = 1$ of the box. As a result, this resonance state is broadened. Figures 7(*c*) and (*d*) demonstrate that two resonance states are broadened when both coupling constants are increased. Also in this case, the two resonance states are shifted beyond the energy band. Such a nonuniform level broadening in the resonance overlapping regime is studied in many different cases by using different approaches, see [9]. It is called resonance trapping [6]. The accompanying shift in energy appears only when the principal value integral of the matrix elements of the effective Hamiltonian is non-vanishing. This is the case in most realistic

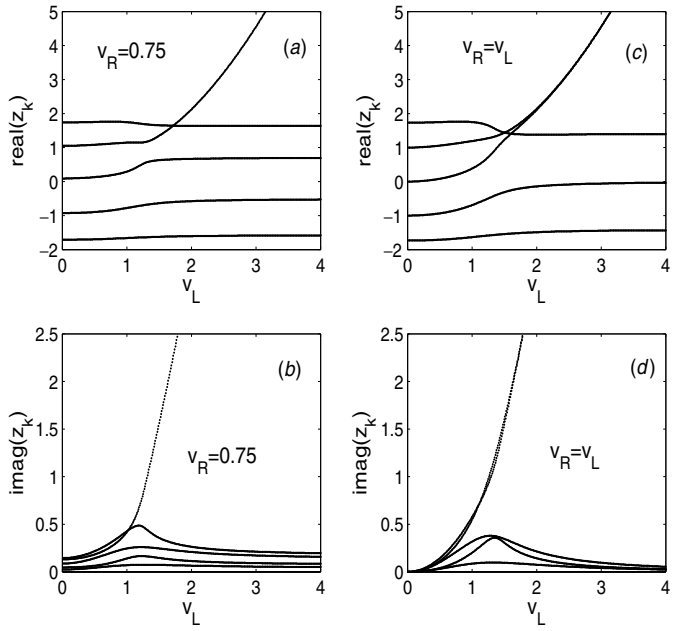

Figure 7. Real and imaginary parts of the five poles of the 1D chain shown in figure 1 versus the coupling coefficients v_L, v_R, $E = 1$. The chain consists of five sites.

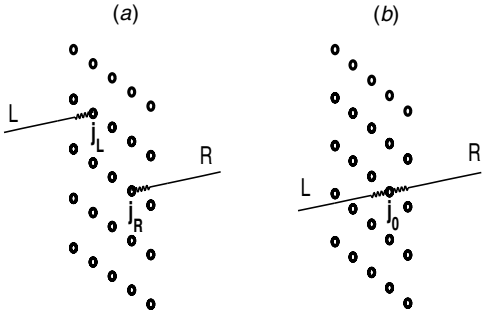

Figure 8. (a) The billiard coupled to left and right 1D leads at the points $\mathbf{j}_L$ and $\mathbf{j}_R$. In (b) $\mathbf{j}_L = \mathbf{j}_R = \mathbf{j}_0$. For simplicity a rectangular billiard is shown in the figure (although it may be of arbitrary shape). The couplings between the billiard and leads v_L and v_R are shown by wavy lines.

systems including atomic nuclei and atoms [9] and also those considered in the present paper (figures 7(a) and (c)).

Thus, the two resonance states do not vanish at strong coupling strength between box and leads as might be concluded from figure 2. The two resonance states go beyond the energy band and can therefore contribute to the transmission only via interference with the remaining narrow resonant states. This example clearly demonstrates the advantage of the effective Hamiltonian approach to the description of transmission.

5.4. Transmission through a 2D billiard connected to 1D leads

Let two 1D leads be coupled to a 2D billiard at the points $\mathbf{j}_L$ (input lead) and $\mathbf{j}_R$ (output lead) where $\mathbf{j} = (j_x, j_y)$, $N_z = 1$ as shown in figure 8(a). Substituting the wavefunctions (15) of

the 1D leads we obtain from equation (56)

$$\langle b|H_{\rm eff}|b'\rangle = E_b\delta_{bb'} + \left[v_L^2\psi_b(\mathbf{j}_L)\psi_{b'}(\mathbf{j}_L) + v_L^2\psi_b(\mathbf{j}_R)\psi_{b'}(\mathbf{j}_R)\right]{\rm e}^{{\rm i}k}. \tag{84}$$

For $\mathbf{j}_L = \mathbf{j}_R$, the equation that defines the poles of the scattering matrix, can be found analytically. From (84) it follows

$$\begin{vmatrix} E_1+\omega\psi_1^2(\mathbf{j}_0)-E & \omega\psi_1(\mathbf{j}_0)\psi_2(\mathbf{j}_0) & \omega\psi_1(\mathbf{j}_0)\psi_3(\mathbf{j}_0) & \dots \\ \omega\psi_1(\mathbf{j}_0)\psi_2(\mathbf{j}_0) & E_2+\omega\psi_2^2(\mathbf{j}_0)-E & \omega\psi_1(\mathbf{j}_0)\psi_3(\mathbf{j}_0) & \dots \\ \omega\psi_1(\mathbf{j}_0)\psi_3(\mathbf{j}_0) & \omega\psi_2(\mathbf{j}_0)\psi_2(\mathbf{j}_0) & E_3+\omega\psi_3^2(\mathbf{j}_0)-E & \dots \\ \vdots & \vdots & \vdots & \dots \end{vmatrix} = 0 \tag{85}$$

where $\omega = \left(v_L^2 + v_R^2\right){\rm e}^{{\rm i}k}$ is the effective coupling constant. The particular case of a 4×4 effective Hamiltonian (85) was considered in [23]. This determinant can easily be transformed to [24]

$$\prod_b \omega\psi_b^2(\mathbf{j}_0)\begin{vmatrix} x_1+1 & 1 & 1 & \dots \\ 1 & x_2+1 & 1 & \dots \\ 1 & 1 & x_3+1 & \dots \\ \vdots & \vdots & \vdots & \dots \end{vmatrix} = \prod_b \omega\psi_b^2(\mathbf{j}_0)\left\{1+\sum_b \frac{1}{x_b}\right\} = 0 \tag{86}$$

where

$$x_b = \frac{E_b - E}{\omega\psi_b^2(\mathbf{j}_0)}.$$

As a result, the equation for the poles of the S-matrix reads

$$\sum_b \frac{\left(v_L^2+v_R^2\right){\rm e}^{-{\rm i}k}\psi_b^2(\mathbf{j}_0)}{E-E_b} = 0. \tag{87}$$

5.5. A 3D billiard connected to a 3D lead

Consider a 3D billiard that has an arbitrary shape in the x, y plane but is restricted in the z-direction by two parallel planes separated by a distance d. In the tight-binding approximation, the height of the 3D billiard can be specified by the number N_z being equal to $1, 2, 3, \dots$. This billiard allows separation of the variables, and is characterized by the eigenvalues and eigenstates of the 3D box Hamiltonian H_B

$$H_B|b_\perp, n_z\rangle = \left(E_{b_\perp} + E_{n_z}\right)|b_\perp, n_z\rangle \tag{88}$$

where $E_{b_\perp}$ are the transverse eigenenergies of the billiard and

$$E_{n_z} = -2\cos\left(\frac{\pi n_z}{N_z+1}\right) \qquad n_z = 1, 2, \dots, N_z \tag{89}$$

are the longitudinal eigenenergies of the box in z-direction. The eigenfunctions in the z-direction are

$$\psi_{n_z}(z) = \sqrt{\frac{2}{N_z+1}}\sin\left(\frac{\pi n_z z_j}{N_z+1}\right) \qquad j_z = 1, 2, \dots, N_z. \tag{90}$$

We consider two different types of the connection between the billiard and the leads that both are shown in figure 9. In the first case, (*a*), the 1D leads are coupled to the billiard at every point $\mathbf{j}$, $j_z = 1$ of the billiard. In the second case, (*b*), the billiard is coupled to the 3D lead the transverse section of which coincides with the shape of the billiard in 2D.

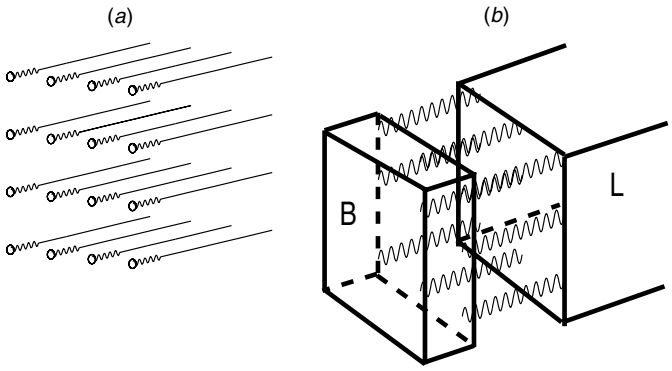

Figure 9. 3D billiards connected to different 3D leads. (*a*) The billiard is coupled to N_b 1D leads at each point $\mathbf{j}$ where N_b is the number of sites of the billiard. (*b*) The billiard is coupled to one 3D lead with the same transverse section as the billiard in 2D. For simplicity, a rectangular billiard is shown although it can be of arbitrary shape. The couplings v between billiard and leads are shown by wavy lines.

For the case (*a*) formula (35) reads

$$Q = E^+ - H_B - \sum_{C=1}^{N_b} V_{BC} \frac{1}{E^+ - H_C} V_{CB} \tag{91}$$

where N_b is the total number of sites of the billiard in the x, y plane. This number is equal to the total number of states $|b\rangle$. The coupling matrix elements are

$$\langle b, n_z | V_{BL} | C \rangle = \sum_{\mathbf{j}_1} \sum_{\mathbf{j}_2} \langle b | \mathbf{j}_1 \rangle \langle \mathbf{j}_1 | V_{BC} | \mathbf{j}_2 \rangle \langle \mathbf{j}_2 | C \rangle = v \psi_b(\mathbf{j}_C) \sqrt{\frac{|\sin k|}{2\pi}} \tag{92}$$

where we assume that the coupling between the billiard and each 1D lead (with the eigenfunction (15)) is equal to v. Substituting (92) into (91) we obtain, similar to (37),

$$\langle b | H_{\text{eff}} | b' \rangle = E_b \delta_{bb'} + \sum_{C=1}^{N_b} \int \mathrm{d}E_1 \, \langle b | V_{BC} | C \rangle \frac{1}{E + \mathrm{i}0 - E_1} \langle C | V_{CB} | b' \rangle = (E_b + v^2 \, \mathrm{e}^{\mathrm{i}k}) \delta_{bb'}. \tag{93}$$

That means, for the case (*a*) in figure 9, the effective Hamiltonian is diagonal with isolated poles $z_b = E_b + v^2 \, \mathrm{e}^{\mathrm{i}k}$, $k = a \cos(-E/2)$.

In the case (*b*) of figure 9, the billiard is coupled to one 3D lead, and the total Hamiltonian is

$$H = H_0 + V$$

$$H_0 = \sum_{b, n_z} \left(E_b + E_{n_z} \right) |b, n_z\rangle \langle b, n_z| + \sum_b \int_{-2+E_b}^{2+E_b} \int \mathrm{d}E \; E [|E, b\rangle \langle E, b| + |b, R\rangle \langle E, b|]$$

$$V = \sum_{bb'} \sum_{nn'_z} \int_{-2+E_{b'}}^{2+E_{b'}} \mathrm{d}E \; V_{b, n_z, b'}(E) |E, b'\rangle \langle b, n_z| + \text{h.c.} \tag{94}$$

where the eigenfunctions of the lead are

$$\langle \mathbf{j}, j_z | E, b \rangle = \sqrt{\frac{1}{2\pi |\sin k_b|}} \sin k_b (1 - j_z) \psi_b(\mathbf{j}). \tag{95}$$

Here, j_z runs along the lead and $\mathbf{j}$ runs over the sites in the transverse section of the lead. Since the transverse section eigenfunctions of the 3D lead coincide with those of the 2D billiard, similar to (63), we have

$$E = -2\cos k_b + E_b. \tag{96}$$

The coupling matrix elements in (94) are

$$V_{b,n_z,b'}(E) = \langle b, n_z|V|E, b'\rangle = \sum_{\mathbf{j},j_z}\sum_{\mathbf{l},l_z}\langle b|\mathbf{j}\rangle\langle n_z|j_z\rangle\langle \mathbf{j}, j_z|V|\mathbf{l}, l_z\rangle\langle \mathbf{l}, l_z|E, b'\rangle. \tag{97}$$

As can be seen from figure 9

$$\langle b|\mathbf{j}, j_z\rangle\langle \mathbf{j}|V|\mathbf{l}, l_z\rangle = v\delta_{\mathbf{j},\mathbf{l}}\delta_{j_z,N_z}\delta_{l_z,1}.$$

Substituting (95) into (97), we get

$$V_{b,n_z,b'}(E) = v\sqrt{\frac{|\sin k_{b'}|}{2\pi}}\sum_{\mathbf{j}}\langle b|\mathbf{j}\rangle\langle \mathbf{j}|b'\rangle\langle N_z|n_z\rangle = v\sqrt{\frac{|\sin k_{b'}|}{2\pi}}\delta_{bb'}\psi_{n_z}(N_z). \tag{98}$$

For the continuous case the last expression has to be substituted by $\psi'(z = d)$ [8]. Therefore, the matrix elements of the effective Hamiltonian are

$$\begin{aligned}\langle b|H_{\text{eff}}|b'\rangle &= \left\{\left(E_b + E_{n_z}\right)\delta_{n_z n_z'} + v^2\psi_{n_z}(N_z)\psi_{n_z'}(N_z)\frac{1}{2\pi}\int_{-2+E_b}^{2+E_b}\mathrm{d}E'\,\frac{\sin k_b}{E + \mathrm{i}0 - E'}\right\}\delta_{bb'} \\ &= \left[\left(E_b + E_{n_z}\right)\delta_{n_z n_z'} + v^2\,\mathrm{e}^{\mathrm{i}k_b}\psi_{n_z}(N_z)\psi_{n_z'}(N_z)\right]\delta_{bb'}.\end{aligned} \tag{99}$$

If $N_z = 1$, we obtain an effective Hamiltonian for the case (b) in figure 9, that is diagonal in the eigen basis of the billiard. This result is similar to that of the case (a). For $N_z > 1$, the effective Hamiltonian is also diagonal, however, with blocks $N_z \times N_z$ at each diagonal place. For $N_z = 2$, taking into account (89) and (90), the matrix block takes the following form

$$H_{\text{eff}} = \begin{pmatrix} E_b + 1 + \frac{v^2}{2}\,\mathrm{e}^{\mathrm{i}k_b} & \frac{v^2}{2}\,\mathrm{e}^{\mathrm{i}k_b} \\ \frac{v^2}{2}\,\mathrm{e}^{\mathrm{i}k_b} & E_b - 1 + \frac{v^2}{2}\,\mathrm{e}^{\mathrm{i}k_b}\end{pmatrix}. \tag{100}$$

Correspondingly, the poles of the S-matrix are

$$z_{n_z,b} = E_b + \frac{v^2}{2}\,\mathrm{e}^{\mathrm{i}k_b} \pm \sqrt{1 + \frac{v^4}{4}\,\mathrm{e}^{2\mathrm{i}k_b}}. \tag{101}$$

Using (96), the condition for the double pole can be written down,

$$v^2 = 2 \qquad E = E_b. \tag{102}$$

6. Wavefunction in the interior of the billiard

The wavefunction in the interior of the billiard is given by expression (34). Using the projection operator for the billiard, $P_B = \sum_b |b\rangle\langle b|$ where $|b\rangle$ are the eigenstates of the (closed) billiard, we can rewrite this expression as follows

$$\psi_B(\mathbf{x}) = \sum_{C,p_C}\sum_{bb'} Q^{-1}_{bb'}V_{b'}(E, C, p_C)\psi_b(\mathbf{x}) = \sum_b f_b\psi_b(\mathbf{x}). \tag{103}$$

The scattering wavefunction in the interior of the billiard can therefore be expanded in the set of eigenfunctions $\psi_b(\mathbf{x})$ of the Hamiltonian of the closed billiard. The expansion coefficients are

$$f_b = \sum_{C,p_C}\sum_{b'} Q^{-1}_{bb'}V_{b'}(E, C, p_C). \tag{104}$$

The drawback of this representation consists in the fact that the expansion (103) includes the procedure of inversion of the matrix (55). Similar to (45) we can use the set of eigenfunctions of the effective Hamiltonian for the expansion of the scattering wavefunction. Using relations (43) and (44) we can write (34) as follows

$$\psi_B(\mathbf{x}) = \sum_\lambda f_\lambda \psi_\lambda(\mathbf{x}) \tag{105}$$

where the expansion coefficients are

$$f_\lambda = \sum_{C,p_C} \frac{V_\lambda(E, C, p_C)}{E^+ - z_\lambda}. \tag{106}$$

7. Summary

In this paper we derived the coupling matrix between a closed billiard and leads attached. The knowledge of the coupling matrix gives the explicit expression for the effective Hamiltonian, the S-matrix and the scattering wavefunction in the interior of the billiard. The non-Hermitian effective Hamiltonian reflects the spectral properties of the closed billiard. The eigenvalues of the effective Hamiltonian however are shifted in energy and are complex because of the openness of the billiard.

The theory presented is based on the tight-binding approach, which allows us to establish the exact correspondence between the S-matrix theory and numerical calculation of the transmission through the billiard that is based on a finite-difference Hamiltonian. The present approach can be easily applied to the continuous case. The advantage of the effective Hamiltonian consists above all in the possibility of interpreting numerical results for the transmission (figure 2) by means of the poles of the S-matrix (figure 7). The last are the eigenvalues of the effective Hamiltonian. It allows us therefore to systematically control the transmission through billiards. We presented a few specific examples for which the effective Hamiltonian reduces to a complex two by two matrix.

Acknowledgments

We thank Konstantin Pichugin for discussions. This work has been partially supported by RFBR grant 01-02-16077, 03-02-17039 and the Royal Swedish Academy of Sciences. AFS also thanks Max-Planck-Institut für Physik komplexer Systeme for its hospitality.

References

[1] Doron E, Smilansky U and Frenkel A 1990 *Phys. Rev. Lett.* **65** 3072
[2] Stöckmann H J 1999 *Quantum Chaos: An Introduction* (Cambridge: Cambridge University Press)
[3] Feshbach H 1958 *Ann. Phys., NY* **5** 357
Feshbach H 1962 *Ann. Phys., NY* **19** 287
[4] Fano U 1961 *Phys. Rev.* **124** 1866
[5] Mahaux C and Weidenmüller H A 1969 *Shell Model Approach in Nuclear Reactions* (Amsterdam: North-Holland)
[6] Rotter I 1991 *Rep. Prog. Phys.* **54** 635
[7] Fyodorov Y V and Sommers H J 1997 *J. Math. Phys.* **38** 1918
[8] Dittes F M 2000 *Phys. Rep.* **339** 215
[9] Okolowicz J, Ploszajczak M and Rotter I 2003 *Phys. Rep.* **374** 271
[10] Šeba P 1996 *Phys. Rev.* B **53** 13024
[11] Albeveiro S, Haake F, Kurasov P, Kuś M and Šeba P 1996 *J. Math. Phys.* **37** 4888

[12] Ohnishi H, Kondo Y and Takayanagi K 1998 *Nature* **395** 780
[13] Yanson A I, Bollinger G R, van den Brom H E, Agraït N and van Ruitenbeck J M 1998 *Nature* **395** 783
[14] Pichugin K, Schanz H and Šeba P 2002 *Phys. Rev.* E **64** 056227
[15] Ando T 1991 *Phys. Rev.* B **44** 8017
[16] Bialynicki-Birula I, Cieplak M and Kaminski J 1992 *Theory of Quanta* (New York: Wiley) ch 19
[17] Ricco B and Azbel Ya 1984 *Phys. Rev.* B **29** 1970
[18] Dittes F M, Harney H I and Rotter I 1991 *Phys. Lett.* A **153** 451
[19] Terraneo M and Guarneri I 2000 *Eur. Phys. J.* B **18** 303
[20] Stöckmann H J, Persson E, Kim Y H, Barth M, Kuhl U and Rotter I 2002 *Phys. Rev.* E **65** 066211
[21] Magunov A I, Rotter I and Strakhova S I 1999 *J. Phys. B: Mol. Opt. Phys.* **32** 1699
[22] Narevicius E and Moiseyev N 2000 *Phys. Rev. Lett.* **84** 1681
[23] Rotter I 2001 *Phys. Rev.* E **64** 036213
[24] Sadreev A F 1978 *Sov. Phys.–JETP* **77** 829